CrossMark

RESEARCH ARTICLE

Differentiating anthropogenic modification and precipitation-driven change on vegetation productivity on the Mongolian Plateau

Ranjeet John · Jiquan Chen · Youngwook Kim · Zu-tao Ou-yang · Jingfeng Xiao · Hoguen Park · Changliang Shao · Yaoqi Zhang · Amartuvshin Amarjargal · Ochirbat Batkhshig · Jiaguo Qi

Abstract

Context The Mongolian Plateau, comprising Inner Mongolia, China (IM) and Mongolia (MG) is undergoing consistent warming and accelerated land cover/land use change. Extensive modifications of water-limited regions can alter ecosystem function and processes; hence, it is important to differentiate the impacts of human activities and precipitation dynamics on vegetation productivity.

Objectives This study distinguished between human-induced and precipitation-driven changes in vegetation cover on the plateau across biome, vegetation type and administrative divisions.

Methods Non-parametric trend tests were applied to the time series of vegetation indices (VI) derived from MODIS and AVHRR and precipitation from TRMM and MERRA reanalysis data. VI residuals adjusted for rainfall were obtained from the regression between growing season maximum VI and monthly accumulated rainfall (June–August) and were used to detect human-induced trends in vegetation productivity during 1981–2010. The total livestock and population

R. John (✉) · J. Chen · Z. Ou-yang ·
H. Park · C. Shao · J. Qi
Center for Global Change and Earth Observations,
Michigan State University, East Lansing, MI 48823, USA
e-mail: ranjeetj@msu.edu

J. Chen · Z. Ou-yang · J. Qi
Department of Geography, Michigan State University,
East Lansing, MI 48823, USA

Y. Kim
Numerical Terradynamic Simulation Group (NTSG)/
College of Forestry and Conservation, The University of
Montana, Missoula, MT 59812, USA

J. Xiao
Earth Systems Research Center, Institute for the Study of
Earth, Oceans, and Space, University of New Hampshire,
Durham, NH 03824, USA

Y. Zhang
School of Forestry and Wildlife Sciences, Auburn
University, Auburn, AL 36949, USA

A. Amarjargal
Department of Economics, University of the Humanities,
Ulaanbaatar 210620, Mongolia

O. Batkhshig
Institute of Geography, Mongolian Academy of Sciences,
Sukhbaatar, Ulaanbaatar 210620, Mongolia

density trends were identified and then used to explain the VI residual trends.

Results The slope of precipitation-adjusted EVI and EVI2 residuals were negatively correlated to total livestock density ($R^2 = 0.59$ and 0.16, $p < 0.05$) in MG and positively correlated with total population density ($R^2 = 0.31$, $p < 0.05$) in IM. The slope of precipitation-adjusted EVI and EVI2 residuals were also negatively correlated with goat density ($R^2 = 0.59$ and 0.19, $p < 0.05$) and sheep density in MG ($R^2 = 0.59$ and 0.13, $p < 0.05$) but not in IM.

Conclusions Some administrative subdivisions in IM and MG showed decreasing trends in VI residuals. These trends could be attributed to increasing livestock or population density and changes in livestock herd composition. Other subdivisions showed increasing trends residuals, suggesting that the vegetation cover increase could be attributed to conservation efforts.

Introduction

The world's arid/semi-arid biome, which accounts for 41 % of the earth's land area and where 38 % of the human population lives, is vulnerable to ongoing and predicted climate change as well as land degradation (Reynolds et al. 2007; Li et al. 2012). The grasslands of the Mongolian Plateau makes up a major portion of the Eurasian Steppe—the largest, contiguous grassland ecosystem in the world—and are among the few extant grassland ecosystems with a high diversity of grassland species (Bai et al. 2008; Chen et al. 2013). While there have been many studies that describe the vegetation, species diversity, and the effects of environmental stochasticity such as drought and extreme winters on the Mongolian Plateau, there have been relatively few studies on the vulnerability of the Mongolian grasslands to climatic change and anthropogenic modification (Hilker et al. 2014; Chen et al. 2015a). The temperate steppes of the plateau are under increasing pressure from a 2° rise in average temperature, a 7 % reduction in annual precipitation during

the last 70 years (Liu et al. 2013), and an increasing frequency of extreme climatic events in the last three decades (Groisman et al. 2009; Fernández-Giménez et al. 2012; John et al. 2013b; Pederson et al. 2014).

The plateau consists of Mongolia (MG) and Inner Mongolia (IM),—the third largest province-level administrative region in China (Fig. 1). The two entities (i.e., MG and IM) have similar ecosystem types but distinct socio-economic systems, political regimes, ethnic compositions, and divergent land cover/use change trajectories (Qi et al. 2012; Chen et al. 2015b). The major land use on the plateau has historically been herding, but cropland use has increased in certain areas of IM (Dong et al. 2011; John et al. 2013b) and more recently in north central MG (Pederson et al. 2013). Livestock stocking rates increased sharply in MG following the collapse of the former Soviet Union and the loss of state support, which drove migration away from cities (Hilker et al. 2014; Chen et al. 2015b). The level of degradation in the Mongol Steppe is closely linked with abrupt changes in socio-economic policies, leading to a dramatic increase in livestock stocking rates in both MG and IM during the last two decades (Ojima and Chuluun 2008; Li et al. 2012; Liu et al. 2013; Hilker et al. 2014; Chen et al. 2015b). Herders on the plateau have been forced to adapt to extreme weather and market forces by limiting their traditional frequency of transhumance (*otor*), becoming sedentary herders (more common in IM than MG), and diversifying herd composition to minimize risk of livestock mortality, all of which has resulted in increased grazing pressure (Fernández-Giménez 2002; Wang et al. 2013b; Hilker et al. 2014). Extreme climate events like summer drought and extreme winters or *dzud*s, led to the migration of herders to urban areas after record livestock mortality in 2000–2002 (Sankey et al. 2009) and again in 2010 (John et al. 2013b; Hilker et al. 2014). The emergence of a market economy and the recent boom in mining partially explain the internal migration in the 2000–2010 decade, which led to an increase in the urban population, concentrated mostly in the capital city of MG, Ulaanbaatar. Similarly, Deng Xiaoping's reforms of the 1980s ushered in a market economy in IM, where the agricultural collectives were replaced by increased privatization of herding and farming (Chen et al. 2015a, b). The last decade saw the introduction of several grassland conservation measures and green
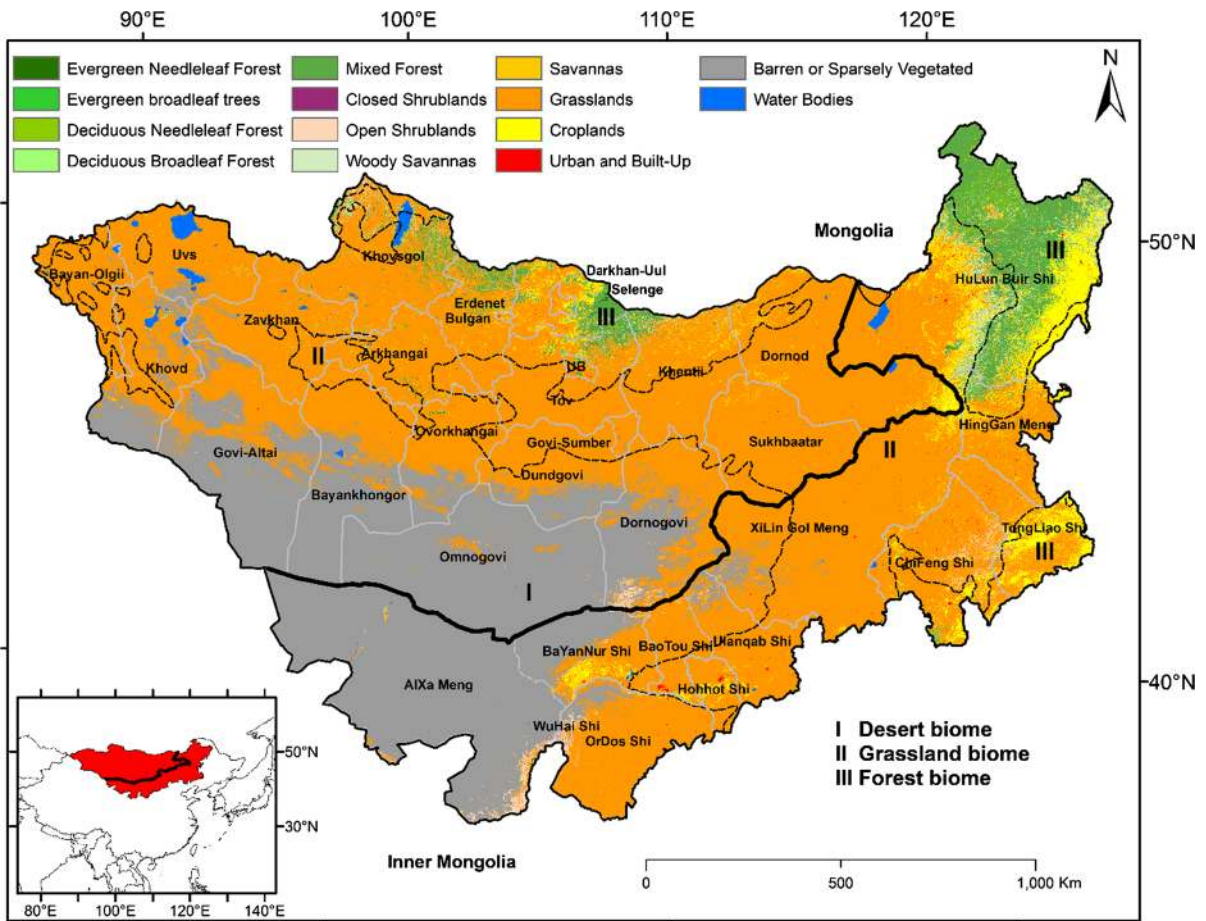
Fig. 1 Land cover map and biome boundaries of the Mongolia Plateau. The base map is the MODIS-derived land cover map with the University of Maryland classification scheme (MCD12Q1) for 2010. The polygons delineated by *dashed lines* are the terrestrial ecoregions (WWF) biome boundaries: desert (I), grassland (II), and forest (III). The heavy, *solid line* stands for the political boundary between Mongolia (MG) and Inner Mongolia (IM), China

belt schemes to control desertification and to mitigate dust storms originating in IM (Jiang et al. 2006; Liu et al. 2008).

The identification of various desertification drivers and the separation of anthropogenic drivers from climatic effects have long been a topic of contention in semi-arid grassland research. Vegetation dynamics in semi-arid grasslands are closely coupled with precipitation variability, which makes it challenging to distinguish degradation resulting from anthropogenic modification from vegetation dynamics in water limited ecosystems (Wessels et al. 2007). Although several satellite remote sensing methods have been used to study vegetation degradation using vegetation indices (VI) (Kim et al. 2014), the primary methods to monitor reduction in grassland canopy cover and

biomass resulting from anthropogenic modification and large inter-annual precipitation variability are to study trends in rain use efficiency (RUE) or spatially explicit residual trends (RESTRENDS) (Wessels et al. 2007). There are few studies that compared residual analysis results across border regions of large extent with similar ecosystem and climate types like the plateau (Zhao et al. 2014) or linked them with socio-economic drivers and policy change (Li et al. 2012; Chen et al. 2015a). Furthermore, there are no studies that compared independent RESTREND results obtained from long-term records of VIs derived from multiple satellite sensors and gridded climate datasets.

In this study, we used RESTREND and multiple VI and climate datasets to examine the effects of anthropogenic modification and precipitation dynamics on

vegetation productivity on the Mongolian Plateau. These state-of-the-art synoptic VI records and climate datasets proved to be valuable for facilitating cross-validation of the results. This method has a secondary utility in monitoring the growth of irrigation agriculture in water-limited areas as well as monitoring grassland degradation from increased grazing pressure. The rationale of this study is to isolate the impacts of anthropogenic modification on grassland vegetation from precipitation driven change in the context of varying land use policies for MG and IM. The study also seeks to measure the rates of change between these political entities owing to differences in market size and human and livestock population density. To facilitate this, it would be necessary to account for the effects of climate drivers, particularly rainfall on vegetation dynamics in water-limited plateau steppes. Our research objectives were to: (1) analyze spatial and temporal trends in long-term satellite-derived VI that were not explained by rainfall dynamics and (2) evaluate socio-economic impacts on changes in satellite-derived VI using trends in total livestock, livestock types, and population density and their relationships with precipitation-adjusted VI residuals.

Methods

Study area

The Mongolian Plateau encompasses an area of 3 million km^2, spanning from 90°E to 130°E longitude and 55°N to 35°N latitude. The plateau includes three major biomes (desert, grassland, forest) and their distribution is mainly determined by the precipitation gradient (Fig. 1) (John et al. 2013b). The climate of the plateau is predominantly semi-arid continental, with warm summers and extremely cold winters. Mean annual temperature ranges from −1.7 °C in the meadow steppe to 5.6 °C in the desert steppe and mean annual precipitation varies from 90 to 433 mm (Fernandez-Gimenez and Allen-Diaz 1999). Most precipitation falls between June through August (JJA), with peak growing season reaching a maximum in August (Li et al. 2012). According to the Köppen-Geiger climate classification, the climate types on the plateau range from a mid-latitude dry semi-arid steppe

climate (BSk) in the southwest where potential evapotranspiration exceeds precipitation and average temperature is less than 18 °C—to a subarctic climate in the northeast with cool summers and severe dry winters (Dwc) (Kottek et al. 2006). Mountain ranges such as the Altai in the west and the Greater Hingaan Mountains in the east isolate the plateau in part from the Monsoon systems. In addition, the Siberian anticyclone controls extreme winter temperature and low precipitation until it weakens with warming in summer (Hilker et al. 2014).

In order to characterize the inter-annual trends of VI, we stratified the plateau into its constituent biomes, vegetation types, and administrative divisions (i.e., aimag in Mongolia and meng in Inner Mongolia). The biome boundaries from the World Wildlife Fund (WWF) terrestrial ecoregions (Olson et al. 2001) dataset were used to stratify the plateau into desert, grassland and forest biomes. In addition, we used a vegetation map (Supplementary Fig. 1) derived from earlier maps produced by the Institute of Botany, Chinese Academy of Sciences (IBCAS, 1990s), and Institute of Botany, Mongolia (1980s) to delineate forest, meadow steppe, typical steppe, desert steppe types (Wang et al. 2013a). The biome boundaries were from WWF Global Ecoregions data while the vegetation maps are more specific and local to the Mongolian Plateau. We conducted analyses based on both data sets as they were independent data sources. We also overlaid the biome boundaries onto the MODIS land cover types to contrast the biomes with the actual land cover/use. North-central Mongolia forms an ecotone between the Siberian boreal taiga and the Central Asian steppe complex and the dominant forest species here are Siberian Larch (*Larix sibirica*) and Siberian Pine (*Pinus sibirica*) (Sharkhuu et al. 2013) with forest cover having lowest proportion among vegetation types (e.g., 10.86 % of Mongolia). The typical steppe vegetation, given a mean annual precipitation (MAP) of 350 mm on the plateau, is composed primarily of C3 grasses with dominant species like *Stipa Grandis, Stipa Krylovi*, and *Cleistogenes* spp, while the desert steppe with a MAP of <150 mm on the plateau is dominated by shrubs (*Caragana* spp, *Artemisa xerophytica* and *Artemisia Ordosia*) (Fernández-Giménez and Allen-Diaz 1999; Cheng et al. 2006; John et al. 2013a). Dominant species of the meadow steppe with a MAP of ≥400 mm are *Stipa Baicalensis, Leymus Chinenis*

and Artemisia frigida (Fernández-Giménez and Allen-Diaz 1999).

Long term satellite data records

The normalized difference vegetation index (NDVI) (Tucker 1979) and enhanced vegetation Index (EVI) (Huete et al. 2002) are commonly used as a proxies for leaf area index (LAI), fractional vegetation cover and gross primary production. The enhanced vegetation Index-2 (EVI2) was developed to provide identical values to the EVI, minimizing potential soil and atmosphere contaminations (Kim et al. 2010). We analyzed the VI trends of the plateau by using three existing long-term VI time series: MODIS EVI (2000–2012), VIP EVI2 (1981-2010), and GIMMS3g NDVI (1981–2010) (Scheftic et al. 2014). The MODIS EVI product consists of monthly composites of 1 km resolution EVI (MOD13A3) from 2000 to 2012 derived from the Moderate Resolution Imaging Spectroradiometer (MODIS) aboard the Terra satellite. The data was downloaded from NASA's Reverb Echo portal (http://reverb.echo.nasa.gov/reverb/). In order to extend the MODIS EVI time series back in time to the 1980s, we obtained EVI2 from the new Vegetation Index and Phenology (VIP) (Didan 2010; Barreto-Munoz 2013) dataset of the NASA MEaSUREs (Making Earth System Data Records for Use in Research Environments) program (http://vip.arizona.edu/viplab_data_explorer.php#). At present, the VIP dataset covers three decades (1981–2010) of consistent EVI2 and NDVI derived from both AVHRR and MODIS with a Climate Modeling Grid (CMG) resolution of 5.6 km (0.05°) (Jiang et al. 2008). The need for cross-validation of the MODIS EVI and VIP EVI 2 datasets motivated us to use NDVI3g, the third generation of GIMMS NDVI derived from all seven AVHRR sensors (Anyamba et al. 2014). State-of-the-art techniques have been used in this latest version of GIMMS NDVI to remove artifacts in the NDVI time series due to differences among sensors, solar zenith angle, and orbital drift.

We used the pixels from the growing season (April–October) with the highest quality in our analysis of the three VI products. We made use of standard quality control (QC bits) and LDOPE tools for MODIS EVI (https://lpdaac.usgs.gov/tools/ldope_tools) (Samanta et al. 2012). Similarly, we used the pixel reliability layer in VIP EVI2 to exclude pixels that were gap-filled with estimated VI or the long-term average. For NDVI3g, we used the embedded flags to account for the possibility of false positives from clouds or snow. In addition, we used the quality flags to distinguish original NDVI from gap-filled NDVI pixels which were derived from spline interpolation and which might be contaminated by clouds (Anyamba et al. 2014).

Climate data

We used the merged Tropical Rainfall Measuring Mission (TRMM) data (Huffman et al. 1995) to explain the effects of precipitation variability on vegetation productivity, as approximated by EVI for the period 2000–2012. We used the monthly precipitation rate (3B43 version 7, http://disc.sci.gsfc.nasa.gov/) to characterize precipitation distribution and deficits (Aragão et al. 2007; Anderson et al. 2010). Although our study area is at the northern edge of the TRMM coverage (50°N), the dominant land cover types (grassland and desert biomes) in both IM and MG are well represented by TRMM pixels. In order to obtain high quality, long term precipitation data for 1981–2010, we downloaded total surface precipitation (PRECTOT) (0.5° × 0.667°) of NASA's Modern-Era Retrospective Analysis for Research and Applications (MERRA) from the Goddard Space Flight Center simple subset portal (http://disc.sci.gsfc.nasa.gov/SSW/) (Rienecker et al. 2011).

Population and Livestock Data

In order to explain human-induced changes in vegetation cover and validate the RESTRENDS method, we obtained detailed census data that include total urban and rural population at Level-1 administrative divisions (i.e., province or aimag level in MG and meng or prefecture level in IM). In addition, official estimates of total livestock population and livestock types (e.g., sheep, goat, cattle, and horses) were obtained from the National Statistical Office Yearbooks in MG. Similar data were obtained from statistical yearbooks and meng level authorities in IM (Statistical Bureau of Inner Mongolia 1989–2012). The annual livestock census in IM is collected twice a year (mid-year and end-of-year) whereas in MG, the census is only taken at the end-of-year. Hence we ensured that we used end-of-year data in both MG and

IM for comparative purposes. Livestock and human population densities were obtained by dividing the total population and livestock by the area of aimag or meng,—i.e., the socio-economic data were normalized by area.

Analyses

We applied non-parametric Mann–Kendall (MK) tests to statistically assess whether there is a monotonic upward or downward trend over time on three independent VI time series: MODIS EVI (2000–2012), VIP EVI2, and GIMMS NDVI3 g (1981–2010) (Fig. 2a, c, d). We also used the Theil–Sen non-parametric test for estimating the significance of the trends (Sen 1968). The MK trend tests are not sensitive to outliers, do not assume a normal distribution, and correct for serial autocorrelation which is especially important for dealing with times series of accumulated climate data like seasonal precipitation (de Beurs et al. 2009). The similar non-parametric methods have been successfully used for climate trend studies using satellite VI datasets (Alcaraz-Segura et al. 2010; de Jong et al. 2011; Kim et al. 2014). The sign of the test statistic indicates an increasing (positive) or decreasing (negative) trend while the magnitude indicates the strength of the trend (Wright et al. 2012). We also correlated de-trended time series of EVI, EVI2, and NDVI3g with accumulated precipitation data from TRMM and MERRA PRECTOT (Fig. 2e, f, Supplementary Fig. 6a).

The RESTREND method was applied to distinguish between anthropogenic land degradation from inter-annual precipitation variability (Wessels et al. 2007). This spatially explicit method is based on the premise that the primary productivity of semi-arid and arid ecosystems is positively correlated with precipitation and that the degradation of grasslands leads to reduced vegetation productivity per unit precipitation (Wessels et al. 2007). The method maps pixel-based trends in the residuals obtained from the regression of accumulated rainfall data and VI (Evans and Geerken 2004; Wessels et al. 2007).

Prior to the RESTRENDS analysis, MODIS EVI was resampled to match the 28 km resolution of TRMM, while VIP EVI2 and NDVI3 g were resampled to match the 50 km resolution of MERRA PRECTOT. The VI residuals (i.e., observed VI − predicted VI) were analyzed to detect trends in vegetation

productivity that were not explained by rainfall dynamics over different time periods (2000–2012 and 1981–2010). A decreasing trend in residuals is an indication of grassland degradation that could be attributed to anthropogenic activity such as grazing and urbanization. Increasing residuals trends suggest that vegetation cover and plant vigor may have improved and could be attributed to efforts in conservation (Wessels et al. 2007). This is based on the assumption that other climate factors, particularly elevated air temperature do not play a significant role in vegetation dynamics for water-limited ecosystems on the plateau (Kim et al. 2012; John et al. 2013b). We carried out pixel-based linear regression analyses between maximum annual VI (VI_{max}), a proxy of peak primary productivity, and accumulated seasonal rainfall during the 30-year study period (1981–2010). In order to determine the best regression model fit between VI_{max}—and accumulated rainfall and to better describe the seasonal distribution of rainfall and vegetation growth, we obtained composites of TRMM and MERRA PRECTOT with variable time lags between the start and peak of the growing season. The precipitation composite variables include accumulated precipitation from June through August (JJA) that is representative of the summer peak growing season and precipitation from April through July (AMJJ) that included spring green up and increasing vegetation growth to the months prior to the peak growing season. The three different time series of the residuals (MODIS EVI *vs* TRMM, EVI2 vs. MERRA PRECTOT, NDVI3g vs. MERRA PRECTOT, respectively) were subjected to non-parametric MK trend tests. In addition, *p* value masks were created so that only statistically significant pixels were retained for comparative analyses (supplementary Fig. 2). The higher spatial resolution of the MODIS EVI time series complemented the temporal resolution of the 30-year VIP EVI2 and NDVI3 g datasets.

We used the MK non-parametric trend tests to analyze time-series of population and total livestock densities and the density of major livestock types, and the Theil–Sen method for slope estimation for the study period. We then mapped the distribution of slope trends in order to explain the variance and distribution of the residual trends of EVI, EVI2, and NDVI3g. Finally, the changes in stocking rate of total livestock and animal types and the human population densities were regressed against the slope of residual trends of

2000-2012

(a)

(b)

1981-2010

(c)

(d)

2000-2012

1981-2010

(e)

(f)
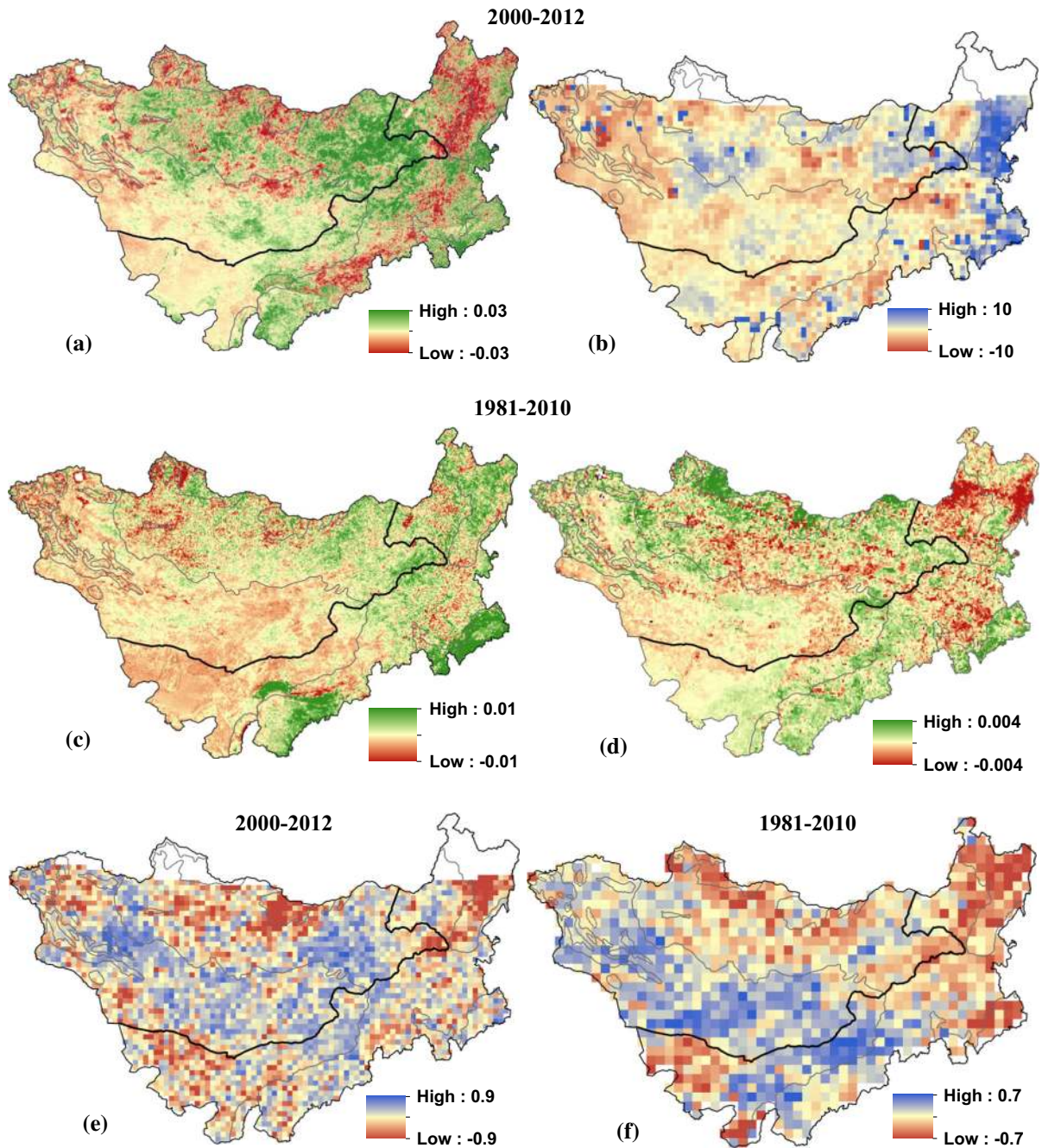
Fig. 2 Spatial distribution of trend slope and correlation between vegetation indices and precipitation for the Mongolia Plateau: **a** trend slope of annual EVI (2000–2012), **b** trend slope of TRMM rainfall (mm year^{-1}), **c** trend slope of annual EVI2 (19810–2010), **d** trend slope of NDVI (1981–2010), **e** correlation between EVI and TRMM precipitation, **f** correlation between EVI2 and MERRA precipitation

the three VI time series. We used Geoda (https://geodacenter.asu.edu/), a spatial regression package, to account for spatial autocorrelation through the use of a spatial lag term which uses weights based on a threshold of the smallest Euclidean distance between all aimags/mengs with at least one neighbor.

2000-2012

(a)

1981-2010

(b)

1981-2010

(c)

High : 0.005

Low : -0.005

0   500   1,000 Km
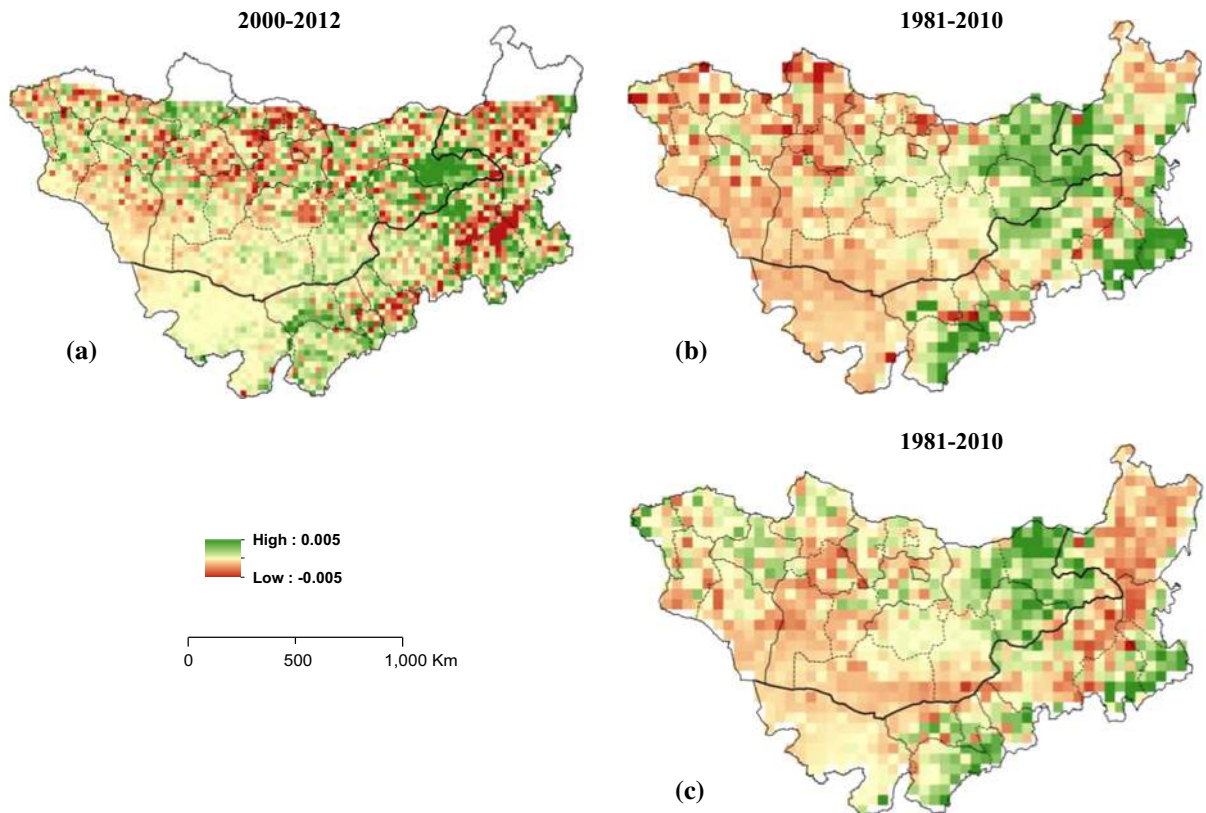
Fig. 3 Residual trends of rainfall-adjusted residuals obtained from linear regression of **a** maximum EVI and accumulated TRMM precipitation in June, July, August (JJA), **b** from regression of maximum EVI2 and accumulated MERRA precipitation in JJA and **c** from regression of maximum NDVI with accumulated MERRA precipitation. EVI, EVI2, and NDVI time series were corrected for the effects of precipitation and the trends here are not explained by precipitation

Results

Relationship between VI$_{max}$ and Rainfall

Precipitation was significantly correlated with MODIS EVI for the dominant desert (correlation coefficient (r) = 0.26–0.39) and grassland biomes (r = 0.31–0.32) (p < 0.05, Supplementary Table 1). In comparison, precipitation showed low correlation with VIs for the forest biome (r = 0.12–0.16), suggesting that the ecosystems in the northern regions of the plateau in both MG and IM were mainly controlled by temperature. Similarly, VIP EVI 2 was also correlated with precipitation for desert (r = 0.18–0.31) and grassland (r = 0.24 and 0.18) in IM and MG, respectively. VIP EVI2 and GIMMS NDVI3 g showed relatively lower correlation with precipitation in the forest biome with −0.15 to 0.07 in IM and 0.12 in MG.

MODIS EVI and TRMM rainfall were positively correlated for the desert biome, and to a certain extent for the grassland biome, in the western and central portions of the plateau over the last decade (Fig. 2e). There was also a strong, negative correlation between EVI and rainfall in the forest biome, especially in northern MG and northeastern IM. EVI2 and MERRA PRECTOT also showed a strong, positive correlation for the desert biome in IM and MG (Fig. 2f). However, there was a strong, negative correlation between precipitation and VIs for the IM forest biome, especially in the southeastern basin through which the Yellow River flows and where the land use is mostly irrigated cropland (Fig. 1). The Hingaan Mountain region of northeastern IM and northern MG, comprising of a mixture of forest cover and agricultural land use, also showed a strong, negative correlation with precipitation (Fig. 1).

We repeated the correlation analysis across vegetation types and found that all three growing season VI of northern forests were negatively correlated with precipitation. The growing season VI of the meadow steppe showed moderate to high correlation for MODIS EVI (r = 0.24–0.42) and GIMMS3 g (r = 0.16–0.24) in IM and MG, respectively (supplementary Table 2). The VIs of the dominant steppe were highly correlated (for e.g., MODIS EVI, r = 0.34–0.41) with precipitation. Similarly, for the desert steppe, the growing season precipitation was correlated with the VIs (MODIS EVI: r = 0.45 and 0.35; VIP EVI2: r = 0.41–0.30; GIMMS3g: r = 0.50–0.15) in IM and MG, respectively (Supplementary Table 2).

Residual trends in precipitation adjusted VI

Trends of the residuals (p < 0.05) obtained from the three VI-precipitation regressions were stratified by the WWF biome types. For the desert biome, the pixels with a decreasing trend in MODIS EVI residuals occupied 8.7 and 23.43 % of the area, whereas the pixels with an increasing trend occupied 15.9 and 27.22 % in IM and MG, respectively (Table 1). Similarly, for the grassland biome, pixels with decreasing trends in residuals occupied 16.45 and 16.84 %, while pixels with increasing trends occupied an area of 21.89 and 24 % in IM and MG, respectively (Table 1). For the forest biome, areas with decreasing

trends in residuals occupied a greater proportion in MG than in IM, while areas with increasing trends were similar to each other (Table 1).

MODIS EVI residual trends stratified by IBCAS vegetation type showed a slight increase in percentage-area under forest cover in IM than in MG, whereas MG showed a greater proportion of forest cover with decreasing trends (Table 2). The percentage-area covered by meadow steppe showed a decrease of 13.95–14.83 % and an increasing trend of 11 % in both IM and MG (Table 2). The relative changes of the typical steppe in MG were larger than those of IM. The percentage area covered by decreasing and increasing trends of the desert steppe in IM were about the same as that of MG (Table 2).

We found a greater magnitude in EVI trends in the last decade (Fig. 2a) than in the 1981–2010 EVI2 trend (Fig. 2c). The trends of MODIS EVI residuals (Fig. 3a) were also larger than those of EVI2 and NDVI3 g residuals (Fig. 3b, c). Residual trends in all three VI time series (Fig. 3) showed significant increases in the eastern Mongolian aimags of Dornod, Sukhbaatar, and Khentii with an annual increase of 0.05 in the eastern portion of the grassland biome. However, there was a decreasing trend of 0.05 in the central and western portions of the grassland biome in MG including the aimags of Tov, Orkhon, Bulgan, Selenge (Fig. 3) and major cities of Ulaanbaatar, Darkhan, and Erdenet. Similarly, there was an increasing trend in VI residuals in southern and

Table 1 Percentage area covered of pixels with different residual trends for three long-term datasets, MODIS EVI, Vegetation and phenology EVI2 product, and the third generation GIMMS NDVI (p < 0.05) by desert, grassland and forest biome boundaries obtained from the WWF biome boundaries

Biome	Year	Product	IM		MG	
			decr.	incr.	decr.	incr.
Desert	2000–2012	MODIS EVI	8.79	15.91	23.43	27.22
	1981–2010	VIP EVI2	10.68	30.04	17.43	34.86
	1981–2010	GIMMS3G NDVI	20.69	22.03	19.21	22.05
Grassland	2000–2012	MODIS EVI	16.45	21.89	16.84	24.01
	1981–2010	VIP EVI2	3.19	15.51	2.90	5.81
	1981–2010	GIMMS3G NDVI	17.79	20.53	6.53	14.52
Forest	2000–2012	MODIS EVI	3.81	6.58	17.55	8.31
	1981–2010	VIP EVI2	6.63	12.15	19.15	10.31
	1981–2010	GIMMS3G NDVI	2.21	7.73	13.26	16.20

Increasing trends signify increased vegetation cover and decreasing trends represent reduced vegetation cover and degradation

Table 2 Percentage area covered of pixels with different residual trends for three long-term datasets, MODIS EVI, vegetation and phenology (VIP) product, and the third generation GIMMS NDVI (p < 0.05) by vegetation types delineated by the Institutes of botany in China (IBCAS) and Mongolia

Vegetation type	Year	Product	IM		MG	
			decr.	incr.	decr.	incr.
Forest	2000–'12	MODIS EVI	2.85	4.75	8.22	1.17
	1981–'10	VIP EVI2	1.52	12.13	11.24	0.0
	1981–'10	GIMMS3G NDVI	4.55	6.06	0	14.98
Meadow steppe	2000–'12	MODIS EVI	13.95	11.16	14.83	10.74
	1981–'10	VIP EVI2	5.93	16.31	2.45	4.08
	1981–'10	GIMMS3G NDVI	17.80	8.90	4.89	9.78
Typical steppe	2000–'12	MODIS EVI	17.81	22.63	27.30	31.34
	1981–'10	VIP EVI2	2.96	13.01	8.06	10.75
	1981–'10	GIMMS3G NDVI	13.61	24.85	11.28	17.73
Desert steppe	2000–'12	MODIS EVI	23.72	32.19	26.35	29.35
	1981–'10	VIP EVI2	16.21	59.43	15.71	35.52
	1981–'10	GIMMS3G NDVI	45.92	48.63	21.18	33.47
Desert	2000–'12	MODIS EVI	5.06	10.97	21.16	15.25
	1981–'10	VIP EVI2	10.76	23.31	18.14	32.65
	1981–'10	GIMMS3G NDVI	15.24	12.55	16.69	9.43

Increasing trends signify increased vegetation cover and decreasing trends represent reduced vegetation cover and degradation

southeastern portions of IM including parts of the Bayanuur, Baotou, Chifeng, and Tongliao mengs. There was also a decreasing residual trend in south-central and northern IM in parts of Hohhot, as well as the mengs of Ulanqab, Xilinhot, Chifeng, Tongliao, and Hulunbuir (Fig. 3).

Trends in anthropogenic drivers

The total livestock density showed a strong positive trend in north-central and western MG including the aimags with the three largest cities, Ulaanbaatar (UB), Erdenet, and Darkhan-Uul (z statistic: 5.1, 6.5 and 5.7) as well as Bulgan, Govisumber, and Arkhangai (z statistic: 5.7, 3.4 and 5.6) (Fig. 4a). These images were dominated by either meadow or typical steppe. Moderate to weak increasing trends in livestock density were found in Dornod and Khentii (z statistic: 0.3 and 3.2) in the meadow/typical steppe as well as in provinces in the desert steppe along the Gobi Desert including Dornogovi, Omnogovi, Bayankhongor and Govi-Altai (z statistic 1.5, 3.4, 2.0 and 3.2). Similarly, the mengs with large cities and towns in IM, like Hohhot, Bayan Nur, Ulanqab (z statistic: 5.0, 6.8, 4.5) of the desert steppe and Tongliao and Hingaan (z statistic: 4.6 and 6.3) of the meadow steppe in the south-central and south-east showed strong positive trends in total livestock density. On the other hand,

mengs like Alxa (z statistic: 2.3) in the desert steppe had moderate to weak increasing trends in livestock density.

Strong positive trends were also found for goat density in the aimags with the three major cities in MG, Erdenet, Ulaanbaatar, and Darkhan-Uul (z statistic of 7.3, 7.0 and 6.9, respectively), all of which are in the meadow/forest steppe (Fig. 4b). Dornod aimag in the east as well as Dornogovi and Omnogovi in the desert steppe in southern MG had moderate to weak increasing trends in goat density. In contrast, increasing trends of goat density in IM were concentrated in the mengs with major cities in the desert steppe such as Ordos, Bayan Nur, and Wuhai (z statistic of 4.12, 6.2 and 5.3, respectively) and the mengs such as Tongliao, Chifeng, and Hingaan (z statistic: 6.6, 5.7 and 6.4, respectively) in the typical/meadow steppe to the east. Notably, moderate to low increasing trends in goat density were observed in the typical steppe of Xilingol, the meadow steppe of Hulunbuir, and in desert steppe of Alxa.

Increasing trends of sheep density in IM were concentrated in the desert steppe meng of Bayan Nur in south-central IM (z statistic = 6.85), and also in the meadow steppe of the Hingaan (z statistic = 6.05). There were moderate to strong increasing trends of sheep density in Xilingol, Ulanqab, and Hulunbuir and decreasing trends in the desert steppe of Baotou and
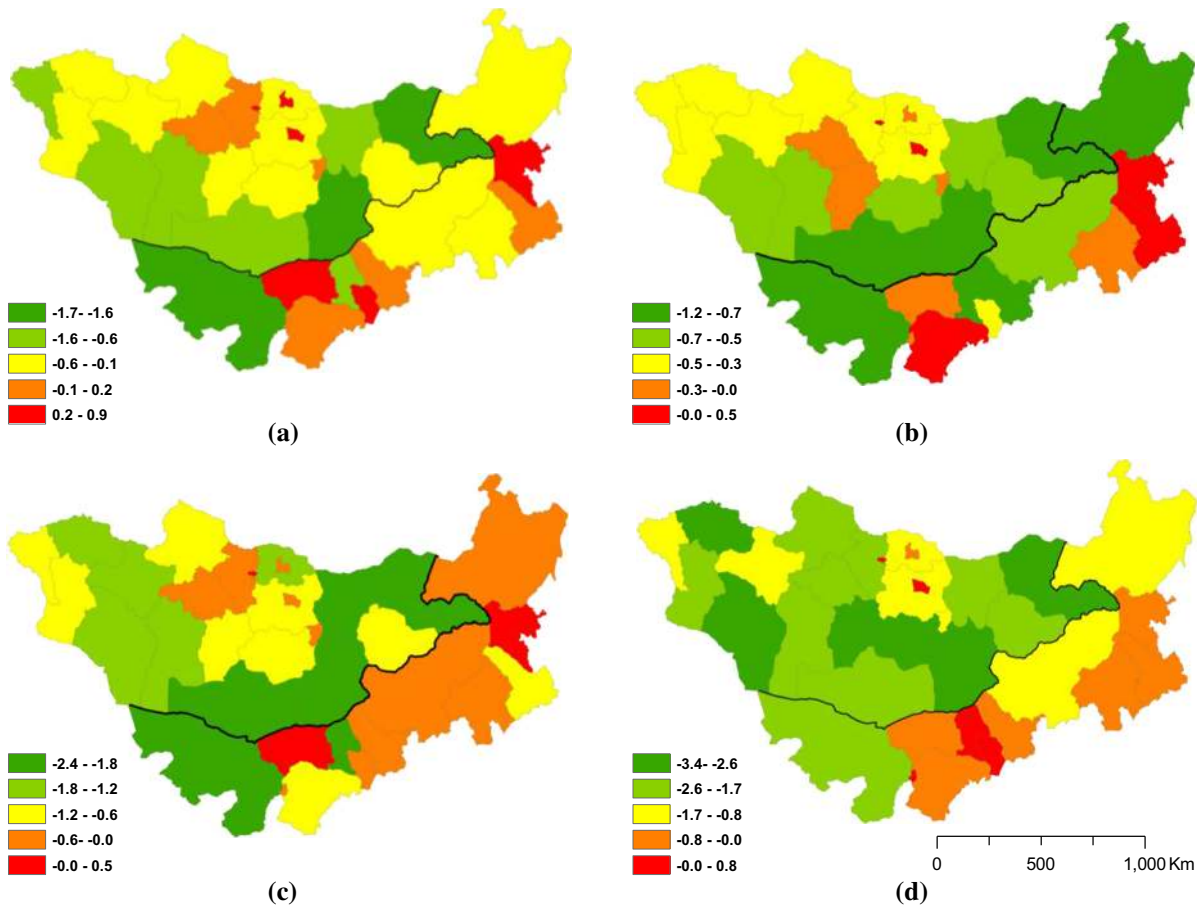
Fig. 4 Slope trends of **a** total livestock density, **b** goat livestock density, **c** sheep livestock density and **d** total population density. The legend shows slopes normalized by log scale

Alaxa (z statistic:−2.4 and −4.5). Increasing trends in sheep density in MG were found in Ulaanbaatar, Darkhan Uul, and Erdenet (z statistic: 3.6, 4.5, and 5.5 respectively) in the meadow/forest steppe. On the other hand, decreasing trends of sheep density in MG were found in the typical steppe of Dornod aimag in the east (z statistic: −2.2), Dornogovi, and Govi-Altai in the desert steppe in the south (z statistic: −4.3 and −2.8), and Khovd and Bayan Olgii in the west (z statistic: −2.3 and −3.6).

Population density in IM showed strong increasing trends in mengs with large cities such as Baotou and Hohot (z statistic: 7.4 and 7.71) in the south-central desert steppe and south-east agricultural basin of Tongliao and Chifeng (z statistic: 6.9 and 5.3), and moderate trends in Xilinhot, Hulunbuir in the typical/ meadow steppe (z statistic: 7.0 and 2.7) and Alxa (z

statistic of 7.0) in the desert steppe. Interestingly, |the peripheral aimags in MG like Dornod in the eastern typical steppe and Dornogovi and Omnogovi in the desert steppe along the Gobi showed a decreasing trend, while there was a strong positive trend in the cities of Ulaanbaatar, Erdenet, and Darkhaan Uul (z statistic: 7.6, 5.7 and 6.4) in the meadow/forest steppe of north-central MG.

Relationships between anthropogenic drivers and VI residual trends

The trends of EVI residuals and trends of total livestock density showed a significant negative correlation in MG ($R^2 = 0.59$, $p < 0.05$) but not in IM ($p > 0.05$). Trends of EVI2 residuals and total livestock density were also negatively correlated for

Table 3 Spatial regression model for June July–August (JJA) EVI, EVI2 and NDVI with livestock and population density in Mongolia

Dependent variable	Independent variables				Goodness of fit	
	Endogenous spatial effects	Livstkd	Popd	Intercept	AIC	Log likelihood
EVI JJA	0.568***	−.0004***		0.0004**	−250.43	128.21
	0.549		−.000	0.000	−231.00	118.50
EVI2 JJA	0.664***	−0.000		0.000	−255.05	130.52
	0.718***		−.000***	0.0002*	−260.26	133.13
NDVI JJA	0.518***	−0.000		0.000	−270.03	138.01
	0.532***		0.000	0.000	−270.88	138.44

*** $p < 0.01$, ** $p < 0.05$, * $p < 0.10$

MG ($R^2 = 0.16$, $p < 0.05$) but not for IM (Fig. 6a, b). We did not find significant correlations between the trends of NDVI3g residuals and total livestock density for either MG or IM. There was significant positive correlation between trends of EVI residuals and trends of population density in IM and MG ($R^2 = 0.31$ and 0.16, $p < 0.05$). EVI and EVI2 residuals did not have any significant relationships with population density due to the sparse demographic distribution in MG. Even though there was some difference in population density among aimags, it was not statistically significant (Fig. 6c, d).

EVI residual trends showed a significant negative correlation with both sheep and goat density trends in MG ($R^2 = 0.59$ respectively, $p < 0.05$) but not in IM (Fig. 7a, c). Trends in EVI2 residuals also showed a significant negative correlation with goat density in MG ($R^2 = 0.20$, $p < 0.05$) (Fig. 7d). However, trends in sheep density were not correlated with EVI2 residual trends in either IM or MG (Fig. 7d). NDVI3g residual trends did not show any significant relationships with increasing goat and sheep density.

Spatial regression between anthropogenic drivers and residual trends

We found significant spatial autocorrelation in regression model fit between our VI residual trends and anthropogenic drivers in MG but not in IM. Statistically significant Moran's I values were the lowest for EVI JJA (0.37) and the highest for EVI2 JJA (0.55) in MG (Supplementary Table 3). While the residuals of the initial regression of VI residual trends with total

livestock density and population density in MG were spatially autocorrelated, the spatial regression model including a spatial lag term removed the effects of spatial autocorrelation. Similar to the previous regression model in MG, the spatial regression model for EVI JJA showed a significant negative correlation with total livestock density but not with population density. On the other hand, EVI2 JJA showed a significant negative correlation with population density but not with livestock density (Table 3). Spatial regression models of goat and sheep density showed significant negative correlation with EVI JJA but not with EVI2 JJA.

Discussion

Vegetation residual trends on the Mongolian Plateau

The importance of semi-arid biomes to global carbon cycling owing to the higher carbon turnover rates emphasizes the continued need for detailed study and monitoring of these water-limited, fragile ecosystems at landscape and regional scales (Qi et al. 2012; Poulter et al. 2014). Recent studies showed that the record 2011 global carbon sink anomaly was largely driven by the growth of semi-arid ecosystems in the southern hemisphere in response to consecutive seasons of increased precipitation caused by the *La Nina* (Poulter et al. 2014). However, the detection and monitoring of grassland degradation is a contentious topic owing to the wide range of methods used,

different types of VI used, and different sources of data. As a result, studies using moderate to coarse resolution VIs and precipitation data often provide contrarian viewpoints on the relationship between precipitation and primary productivity as measured by VIs in the *Sahel* (Xiao and Moody 2005; Prince et al. 2007; Hein et al. 2011).

Several vegetation trend analysis studies in the recent past have reported increased primary production between the 1980s and 1990s (Xiao and Moody 2004, 2005; Piao et al. 2006), whereas other studies found a 16 % decline in vegetation cover (Park and Sohn 2010). However, field observations studies have recorded strong evidence for an increase in grassland degradation as a result of overgrazing (Jiang et al. 2006). Therefore, there is a need for more grassland degradation studies to isolate climatic effects, especially precipitation in water-limited ecosystems like the semi-arid Mongolian grasslands, before drawing conclusions from trends in VI time series.

The residual trends across the plateau were heterogeneous because of the spatial variability in climate and socio-economic drivers (Chen et al. 2015a). Increasing residual VI trends adjusted for rainfall over the past three decades in southwestern IM could be attributed to the increased irrigated croplands and drawdown from the Huang He River in the Hetao irrigation basin in Linhe County, Bayan Nuur (John et al. 2009). Similarly, the increasing trends in Tongliao and Chifeng of southeastern IM could be explained by irrigation agriculture practices, as VI trends in this agricultural basin and the aforementioned Hetao irrigated basin were negatively correlated with rainfall (Fig. 2f), but had increasing trends in annual MODIS-derived evapotranspiration (ET) from 2000 to 2012 (Supplementary Fig. 6b). The increasing ET trends in the same area as increasing residual VI trends were likely caused by an increase in cropland cover and were in close proximity to the rapidly increasing urban population in the cities of Baotou and Hohhot as well as Tongliao and Chifeng (Runnström 2000). In addition, an increase in vegetation trends could also be attributed to grassland conservation in Ordos (Runnström 2000; Zhao et al. 2014). However, decreasing residual VI trends in east-central IM have been attributed to degradation, owing to abandoned croplands in the typical/meadow steppe matrix in Xilingol (Kawada et al. 2011). Decreasing trends in southwestern IM could be also explained by

the rapid increase in cities like Hohhot and Baotou in the desert/typical steppe ecotone.

Increasing residual trends in eastern MG were also found by other studies (Hilker et al. 2014) and can be partially explained by the decreasing trend in both total livestock and population density in aimags in the east (e.g., Dornod). Another reason for increasing residual trends could be the "Atar-3" or Crop-3, a.k.a., "The third campaign for reclaiming virgin lands" development program, initiated by the Mongolian Government with increased spending between 2005 and 2009 in order to increase food security and prevent food crises after the prolonged 2000–2002 drought (Pederson et al. 2013). This might explain increasing trends in Tov, Bulgan, and Selenge, near the major cities in MG. Decreasing residual trends in north-central and western MG can be explained in part by the growth of the three largest cities in MG and the increase in herd size (Fig. 4). Our results are corroborated by similar studies which found a cumulative increase in herd size in western MG (Hilker et al. 2014) and an increase in goat density in central Mongolia (Liu et al. 2013).

The differences between higher resolution residual trends derived from TRMM and MODIS EVI and coarser resolution residual trends derived from EVI2 or NDVI3g and MERRA PRECTOT (Fig. 3) should be interpreted with caution. In addition to changes in precipitation (Fig. 2b), an increasing warming trend might explain some of decrease in residuals trends, especially in the desert steppe in MG (Hilker et al. 2014) as well as in northeastern IM. Precipitation was highly correlated with VIs in the desert steppe, typical steppe and meadow steppe (Supplementary Table 1). However, the plateau has 20° of latitudinal extent (35 N to 55 N) with a significant portion of its northern extent that is limited by temperature rather than precipitation. Significant warming of the plateau could cause the greening of northern meadow and forest steppe but might also limit soil moisture in the desert steppe (Poulter et al. 2013).

Policy shifts, livestock composition, and land use change as socio-economic drivers

The 1980s in IM could be characterized by a slow transition from a collective economy to a market economy under the Deng Xiaoping reforms, which abolished agricultural collectives (Fig. 5,

Supplementary Fig. 4). The 1990s saw the collapse of the former Soviet Union, and with it, the loss of economic support to MG (Qi et al. 2012). Growing unemployment, stemming from the suspension of government jobs, led to an outmigration of people from urban to rural areas. These people then turned to subsistence herding, resulting in a dramatic increase in livestock stocking rates in MG and thereby increased grazing pressure (Fig. 5, Supplementary Fig. 4f) (Sankey et al. 2009; Hilker et al. 2014; Chen et al. 2015b). The same decade saw the emergence of a mature market economy driven by the household production responsibility system in IM. Large-scale grassland degradation has been attributed to the increased privatization of herder families (Li et al. 2012) which led to a sharp increase in livestock stocking rates and subsequent grazing pressure (Fig. 5, Supplementary Fig. 4). The 2000s saw the implementation of grassland conservation policies in response to the severe drought of 2000–2002 in IM (Li et al. 2012; John et al. 2013b), while Mongolian policy directed the increase in cropland extent (Pederson et al. 2013). The rate of change in livestock in IM showed a sudden dip around 2008–2009 likely because of the

global financial crisis of 2008, which led to a 7.33 % decrease in GDP in the first half of 2009 (Fig. 5) (Yuan et al. 2010; Chen et al. 2015b). It is possible that the drop in demand in international and domestic markets for cashmere products reduced goat density in IM. Both MG and IM were affected by the combined effects of drought-dzuds in 2000–2002 and 2010 (John et al. 2013b), although the free range livestock in MG was affected more than that in IM, as they had infrastructure available to shelter livestock (Fig. 5a, b).

Our livestock trends were consistent with previous results (Sankey et al. 2009; Hilker et al. 2014; Chen et al. 2015b) showing sharp increases in sheep and goat populations (Fig. 6, Supplementary Fig. 4c) relative to the total herd numbers in MG. Spatial trend maps of total livestock density and livestock type agreed with those of previous studies showing increasing trends of cumulative herd size and increasing density in western and north-central regions of MG (Liu et al. 2013; Hilker et al. 2014). The dramatic rise in the goat population was likely due to the adaptive measures taken by herders in both IM and MG to diversify their herds following large-scale livestock
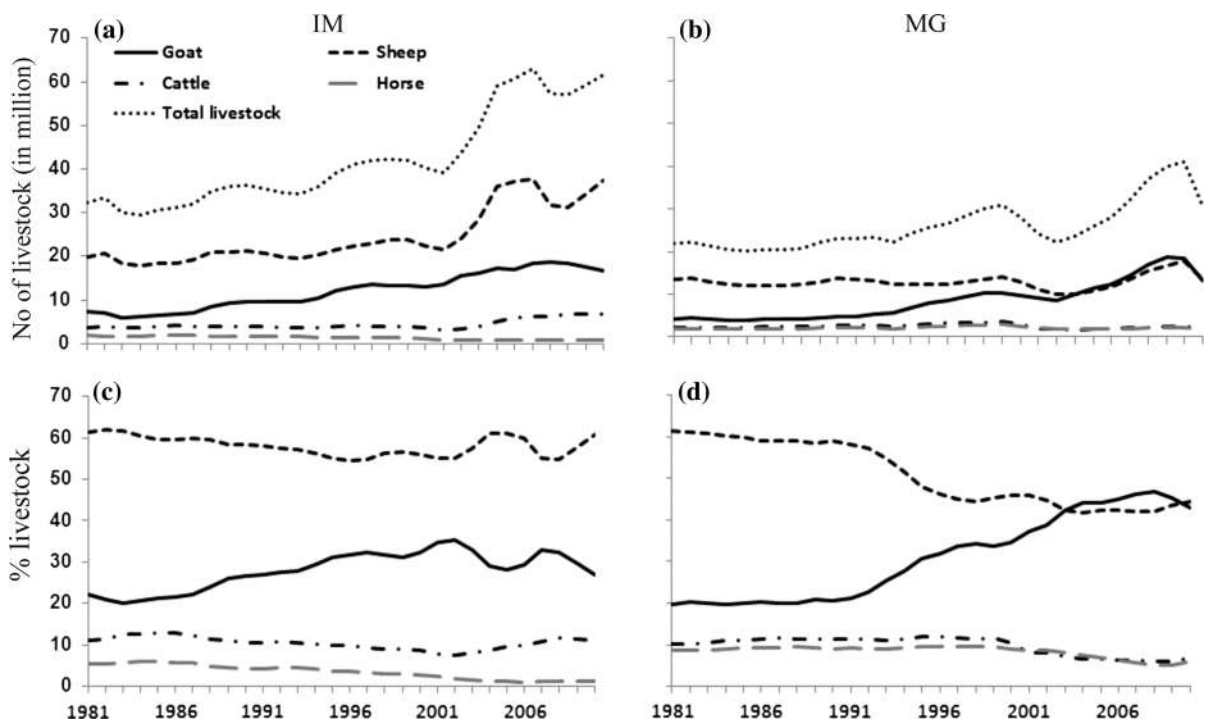
Fig. 5 Temporal trends of total livestock, goat, sheep, cattle, horse and their proportions in Inner Mongolia (IM) (a, c) and Mongolia (MG) (b, d). The figure shows the dramatic proportional increase in goat population in MG and the increase in total livestock in both MG and IM between 1990 and 2010
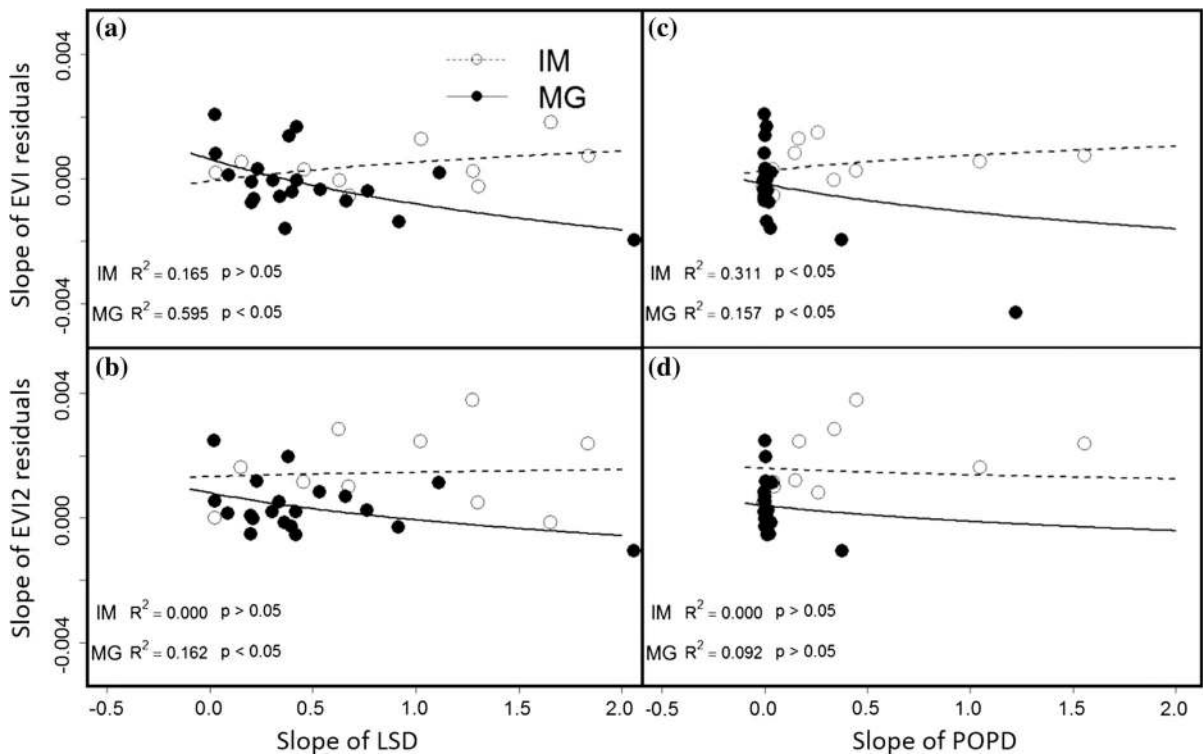
Fig. 6 Relationships of precipitation-adjusted VI residuals with trends in livestock density (LSD) (**a** EVI vs. LSD, **b** EVI2 vs. LSD) and population density (POPD) (**c** EVI vs. POPD, **d** EVI2 vs. POPD) in Mongolia (MG) and Inner Mongolia (IM) at *aimag* and *meng* levels respectively

mortality. The herds were diversified because goats have a greater chance of survival in competing for rangeland resources (Hilker et al. 2014). The steep increase in the market price of cashmere in China and MG and the increase in international demand are also important factors driving the increasing trend in goat livestock density (Sankey et al. 2009; Hilker et al. 2014). This increase of goat livestock type in herd composition has ecological consequences because goats can cause greater grazing degradation compared to sheep herds (Hilker et al. 2014) (Table 4).

The last decade also witnessed increasing urbanization in MG where almost 50 % of the population is concentrated in the capital, Ulaanbaatar, the second largest city (Erdenet), and the second largest industrial center (Darkhan city) (Supplementary Fig. 4e, f). Urbanization in IM cities are mainly centered on Hohhot, Chifeng, Baotou, Tongliao, and cities like Ordos in the desert steppe, which expanded greatly in the last decade because of over-investment and real

estate speculation fueled by the discovery of coal deposits nearby (Runnström 2000). The discovery of mineral deposits and their exploitation by large-scale mining activities might explain the decreasing residual trends not explained by the increase in either livestock or population density (Chen et al. 2015b).

We were able to explain 57 and 27 % of the negative correlation between the trends of VI residuals adjusted for precipitation and the rate of change in total livestock density in MG and IM, respectively. Similar research carried out in IM, albeit in a smaller study area, was able to explain 25 % of the variation in VI residual trends with stocking rate change in nine counties in Xilingol. In addition, a nation-wide study conducted in MG found a significant negative relationship between cumulative changes in herd size and a decline in mean NDVI (2002–2012) in typical and desert steppe, with 70–80 % of variability explained by livestock increase (Hilker et al. 2014). This finding contradicted another nation-wide study in Mongolia

Table 4 Spatial regression model for June July–August (JJA) EVI, EVI2 and NDVI with goat and sheep population density in Mongolia

Dependent variable	Independent variables				Goodness of fit	
	Endogenous spatial effects	Goatd	Sheepd	Intercept	AIC	Log likelihood
EVI JJA	0.562***	−.001***		0.000***	−250.12	128.06
	0.566***		−.001***	0.000	−250.84	128.42
EVI2 JJA	0.662***	−0.000		0.000	−254.95	130.47
	0.665***		−.000***	0.0002***	−255.21	130.60
NDVI JJA	0.517***	−0.000		0.000	−270.15	138.07
	0.519***		−.000	0.000	−269.91	137.95

*** $p < 0.01$, ** $p < 0.05$, * $p < 0.10$

which suggested that climate change explained 60 % of the decline in vegetation with the rest of the variation explained by dramatic increase in goat numbers and by grassland wildfires (Liu et al. 2013). We also found a moderate but significant correlation in residual trends with increasing population density in IM but not in MG. This could be explained by the huge gap in both total and urban populations between IM and MG (supplementary Fig. 4e, f).

RESTRENDS analysis: advantages and drawbacks

Studies in southern Africa found that negative trends were discovered and were most significant when degradation occurred rapidly over a period of 2–6 years (Wessels et al. 2012). Some areas known to be degraded, a priori, were only detected at 10–20 % reduction when compared to non-degraded areas and areas with >20 % reduction caused the RESTRENDs method to become unreliable as the relationship between grassland growth, as detected by VIs and precipitation broke down (Wessels et al. 2012). Long-term droughts combined with increased grazing pressure may severely weaken the intrinsic resilience of grasslands which have a nonlinear relationship with ecosystem structural variables (e.g., vegetation cover) and may increase recovery times (Li et al. 2012). The high level of spatial heterogeneity might explain the weak relationship between VI residual trends and precipitation, especially in the case of IM with increasing road and urban development (Li et al. 2010).

This method is also limited by the coarse resolution of the satellite data (e.g., 28 km TRMM) and gridded climate precipitation products (e.g. 0.5° or 50 km resolution MERRA PRECTOT). While there are many scientifically validated, high quality VI time series available at moderate resolution (500–1000 m EVI, VIP EVI at CMG resolution, or 8 km GIMMS 3g), they have to be resampled to match the coarse resolution of precipitation datasets in order to facilitate per-pixel regression. The spatially-explicit residuals of coarse resolution cannot capture landscape-level trends at finer scales. The recent launch of the global precipitation mission (GPM) will enable future RESTRENDs to be carried out at finer spatial scales.

A major assumption of the RESTRENDs approach is that precipitation is the primary climatic driver in dominant vegetation types (i.e., the typical and desert steppe) and thereby the remaining variance can be attributed to human activities. The semi-arid desert steppe is driven by highly variable precipitation and operates in a non-equilibrium manner (Fernández-Giménez and Allen-Diaz 1999). The meadow steppe, with a lower coefficient of variation in mean annual rainfall conforms to the range control model where grazing density and pressure influence grassland dynamics. The typical steppe—the dominant vegetation type of the Mongolian grasslands—is an ecotone between the desert and meadow steppes and exhibits characteristics common to both. However, temperature might play a significant role in controlling vegetation dynamics even in semi-arid regions like the Mongolian Plateau ("Relationship between VImax and Rainfall" section). The forest and the meadow steppe in the north of the plateau exhibited weak relationships between VIs and precipitation likely because these ecosystems were jointly controlled by rainfall and temperature over the growing season rather than annual precipitation (Figs. 2, 3,
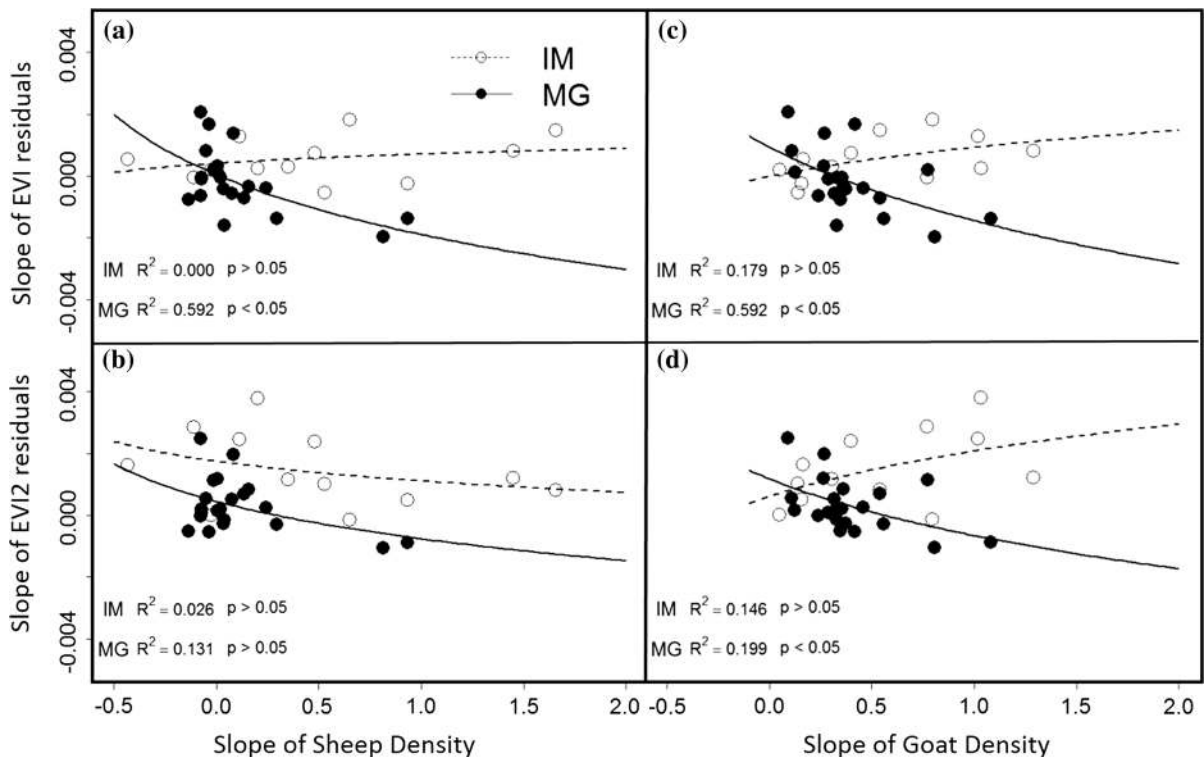
Fig. 7 Relationships of precipitation-adjusted VI residuals with trends in goat density (**a** EVI vs. goat density, **b** EVI2 vs. goat density) and sheep density (**c** EVI vs. sheep density, **d** EVI2 vs. sheep density) in Mongolia (MG) and Inner Mongolia(IM) at *aimag* and *meng* levels respectively

Supplementary Fig. 1) (Liu et al. 2015). In addition, rainfall might not be a limiting factor for the meadow steppe, owing to the high soil moisture along rivers (e.g., the Yellow River in IM or the Kherlen in MG, Figs. 2, 3) or for the forest steppe on the slopes of mountain ranges like the Hingaan mountains with meltwater in spring (Li et al. 2012; Liu et al. 2013).

Rangeland management and traditional transhumance

The Livestock and Rangeland Double-Contract Responsibility System (LRDCRS) in IM, implemented in the late 1980s and continued to the present day, encouraged sedentarization of livestock herders within delimited grazing lands and fixed responsibility on households (Akram et al. 2008). In addition, certain degraded grassland areas were fenced-off and the local herders relocated and resettled as part of the 6-year fencing grassland and moving user's policy (FGMU) (Akram et al. 2008). Sedentary herding could not

replace the preference for traditional transhumance practices like *otor* which provided access to key grazing resources through seasonal migration in an uncertain semi-arid environment with highly variable climate as well as climate adaption strategies like herd diversification (Zhang et al. 2013). A case study in Alxa Left Banner in IM showed that with 25,000 herders relocated to farmlands irrigated with water from the Yellow River or from ground water, privatization and the ecological resettlement of nomadic herders led to major changes in lifestyle owing to increased household income. However, this had the unintended effect of increased water usage leading to water shortages and increased production costs that were not sustainable in a water-limited ecosystem (Fan et al. 2015). The negative relationship between total livestock density and vegetation cover trends in MG indicated that moderate control of livestock stocking rates might alleviate grazing pressure. It is important to incorporate traditional herding knowledge of transhumance and community-based climate

adaption strategies when formulating future legislation and rangeland policies, especially in the typical and desert steppe with their highly variable climate (Fig. 7).

Conclusions

We assessed the magnitude and extent of precipitation-adjusted VI residual trends obtained from satellite-derived VI time series (MODIS EVI, VIP EV2, and NDVI3g) and precipitation data from TRMM and MERRA across biomes and vegetation types in both IM and MG on the plateau. We found significant differences in the extent of increasing and decreasing trends, which were unique in both the decadal (MODIS, 2000–2012) and the 30-year (EVI2, NDVI3g) satellite-based VI records. Our results showed that VI residual trends not explained by precipitation exhibited a significant negative correlation with increasing trends of total livestock density in MG but not IM. Finally, we were able to evaluate our results at different temporal scales and across different datasets. Our 30-year EVI2 precipitation-adjusted residual trends helped confirm differential responses found in the 13-year MODIS EVI record. Our results suggest that future grazing and land use policies revisit the current sedentary practices and accommodate traditional transhumance practices that evolved from the highly variable climate of the semi-arid steppe on a case-by-case basis depending on the level of degradation. There is a need for further investigation into identifying and isolating the possible socio-economic drivers of land use change such as urban expansion, increase in irrigated crop cover or climate drivers like temperature that might influence variability in precipitation-adjusted residual trends.

References

Akram M, Qian Z, Wenjun L (2008) Policy analysis in grassland management of Xilingol Prefecture, Inner Mongolia in. In: Lee C, Schaaf T (eds) The future of drylands. Springer, Dordrecht, pp 493–505

Alcaraz-Segura D, Liras E, Tabik S, Paruelo J, Cabello J (2010) Evaluating the consistency of the 1982–1999 NDVI trends in the Iberian Peninsula across four time-series derived from the AVHRR sensor: LTDR, GIMMS, FASIR, and PAL-II. Sensors 10(2):1291–1314

Anderson LO, Malhi Y, Aragão LEOC, Ladle R, Arai E, Barbier N, Phillips O (2010) Remote sensing detection of droughts in Amazonian forest canopies. New Phytol 187(3):733–750

Anyamba A, Small J, Tucker C, Pak E (2014) Thirty-two years of Sahelian zone growing season non-stationary NDVI3g patterns and trends. Remote Sens 6(4):3101–3122

Aragão LEOC, Malhi Y, Roman-Cuesta RM, Saatchi S, Anderson LO, Shimabukuro YE (2007) Spatial patterns and fire response of recent Amazonian droughts. Geophys Res Lett 34(7):L07701

Bai Y, Wu J, Xing Q, Pan Q, Huang J, Yang D, Han X (2008) Primary production and rain use efficiency across a precipitation gradient on the Mongolia Plateau. Ecology 89(8):2140–2153

Barreto-Munoz A (2013) Multi-sensor vegetation index and land surface phenology earth science data records in support of global change studies: data quality challenges and data explorer system. The University of Arizona, Tucson

Chen J, Wan S, Henebry G, Qi J, Gutman G, Sun G, Kappas M (eds) (2013) Dryland East Asia (DEA): land dynamics amid social and climate change. HEP and De Gruyter, Berlin, 470 pp. Retrieved 22 Aug 2015, from http://www.degruyter.com/view/product/183249

Chen J, John R, Shao C, Fan Y, Zhang Y, Amarjargal A, Brown DG, Qi J, Han JG, Lafortezza R, Dong G (2015a) Policy shifts influence the functional changes of the CNH systems on the Mongolian Plateau. Environ Res Lett. doi:10.1007/s11367-015-0915-6

Chen J, John R, Zhang Y, Shao C, Brown DG, Batkhishig O, Amarjargal A, Ouyang Z, Dong G, Wang D, Qi J (2015b) Divergences of two coupled human and natural systems on the Mongolian Plateau. Bioscience 65(6):559–570

Cheng X, An S, Li B, Chen J, Lin G, Liu Y, Luo Y, Liu S (2006) Summer rain pulse size and rainwater uptake by three dominant desert plants in a desertified grassland ecosystem in northwestern China. Plant Ecol 184(1):1–12

de Beurs K, Wright CK, Henebry GM (2009) Dual scale trend analysis for evaluating climatic and anthropogenic effects on the vegetated land surface in Russia and Kazakhstan. Environ Res Lett 4(4):045012

de Jong R, de Bruin S, de Wit A, Schaepman ME, Dent DL (2011) Analysis of monotonic greening and browning trends from global NDVI time-series. Remote Sens Environ 115(2):692–702

Didan K (2010) Multi-satellite earth science data record for studying global vegetation trends and changes. In: International geoscience and remote sensing symposium, Honolulu, pp 25–30

Dong J, Liu J, Yan H, Tao F, Kuang W (2011) Spatio-temporal pattern and rationality of land reclamation and cropland abandonment in mid-eastern Inner Mongolia of China in 1990–2005. Environ Monit Assess 179(1–4):137–153

Evans J, Geerken R (2004) Discrimination between climate and human-induced dryland degradation. J Arid Environ 57(4):535–554

Fan M, Li Y, Li W (2015) Solving one problem by creating a bigger one: the consequences of ecological resettlement for grassland restoration and poverty alleviation in North-western China. Land Use Policy 42:124–130

Fernández-Giménez ME (2002) Spatial and social boundaries and the paradox of pastoral land tenure: a case study from postsocialist Mongolia. Hum Ecol 30(1):49–78

Fernández-Giménez ME, Allen-Diaz B (1999) Testing a non-equilibrium model of rangeland vegetation dynamics in Mongolia. J Appl Ecol 36(6):871–885

Fernández-Giménez ME, Batkhishig B, Batbuyan B (2012) Cross-boundary and cross-level dynamics increase vulnerability to severe winter disasters (dzud) in Mongolia. Glob Environ Change 22(4):836–851

Groisman PY, Clark EA, Lettenmaier DP, Kattsov VM, Sokolik IN, Aizen VB, Cartus O, Chen J, Schmullius CC, Conard S, Katzenberger J, Krankina O, Kukkonen J, Sofiev MA, Machida T, Maksyutov S, Ojima D, Qi J, Romanovsky VE, Walker D, Santoro M, Shiklomanov AI, Vörösmarty C, Shimoyama K, Shugart HH, Shuman JK, Sukhinin AI, Wood EF (2009) The Northern Eurasia Earth Science Partnership: an example of science applied to societal needs. Bull Am Meteorol Soc 90(5):671–688

Hein L, de Ridder N, Hiernaux P, Leemans R, de Wit A, Schaepman M (2011) Desertification in the Sahel: towards better accounting for ecosystem dynamics in the interpretation of remote sensing images. J Arid Environ 75(11):1164–1172

Hilker T, Natsagdorj E, Waring RH, Lyapustin A, Wang Y (2014) Satellite observed widespread decline in Mongolian grasslands largely due to overgrazing. Glob Change Biol 20(2):418–428

Huete A, Didan K, Miura T, Rodriguez EP, Gao X, Ferreira LG (2002) Overview of the radiometric and biophysical performance of the MODIS vegetation indices. Remote Sens Environ 83(1–2):195–213

Huffman GJ, Adler RF, Rudolf B, Schneider U, Keehn PR (1995) Global precipitation estimates based on a technique for combining satellite-based estimates, rain gauge analysis, and NWP Model precipitation information. J Clim 8(5):1284–1295

Jiang G, Han X, Wu J (2006) Restoration and management of the Inner Mongolia grassland require a sustainable strategy. Ambio 35(5):269–270

Jiang Z, Huete AR, Didan K, Miura T (2008) Development of a two-band enhanced vegetation index without a blue band. Remote Sens Environ 112(10):3833–3845

John R, Chen J, Lu N, Wilske B (2009) Land cover/land use change in semi-arid Inner Mongolia: 1992–2004. Environ Res Lett 4(4):045010

John R, Chen J, Noormets A, Xiao X, Xu J, Lu N, Chen S (2013a) Modelling gross primary production in semi-arid Inner Mongolia using MODIS imagery and eddy covariance data. Int J Remote Sens 34(8):2829–2857

John R, Chen J, Ou-Yang Z-T, Xiao J, Becker R, Samanta A, Ganguly S, Yuan W, Batkhishig O (2013b) Vegetation response to extreme climate events on the Mongolian Plateau from 2000 to 2010. Environ Res Lett 8(3):035033

Kawada K, Wuyunna, Nakamura T (2011) Land degradation of abandoned croplands in the Xilingol steppe region, Inner Mongolia, China. Grassl Sci 57(1):58–64

Kim Y, Huete AR, Miura T, Jiang Z (2010) Spectral compatibility of vegetation indices across sensors: band decomposition analysis with Hyperion data. J Appl Remote Sens 4(1):043520-20–043520-22

Kim Y, Kimball JS, Zhang K, McDonald KC (2012) Satellite detection of increasing Northern Hemisphere non-frozen seasons from 1979 to 2008: implications for regional vegetation growth. Remote Sens Environ 121:472–487

Kim Y, Kimball JS, Zhang K, Didan K, Velicogna I, McDonald KC (2014) Attribution of divergent northern vegetation growth responses to lengthening non-frozen seasons using satellite optical-NIR and microwave remote sensing. Int J Remote Sens 35(10):3700–3721

Kottek M, Grieser J, Beck C, Rudolf B, Rubel F (2006) World Map of the Köppen–Geiger climate classification updated. Meteorol Z 15(3):259–263

Li A, Wu J, Huang J (2012) Distinguishing between human-induced and climate-driven vegetation changes: a critical application of RESTREND in inner Mongolia. Landscape Ecol 27(7):969–982

Li T, Shilling F, Thorne J, Li F, Schott H, Boynton R, Berry A (2010) Fragmentation of China's landscape by roads and urban areas. Landscape Ecol 25(6):839–853

Liu J, Li S, Ouyang Z, Tam C, Chen X (2008) Ecological and socioeconomic effects of China's policies for ecosystem services. Proc Natl Acad Sci USA 105(28):9477–9482

Liu YY, Evans JP, McCabe MF, de Jeu RAM, van Dijk AIJM, Dolman AJ, Saizen I (2013) Changing climate and overgrazing are decimating Mongolian steppes. PLoS ONE 8(2):e57599

Liu Y, Zhuang Q, Miralles D, Pan Z, Kicklighter D, Zhu Q, He Y, Chen J, Tchebakova N, Sirin A, Niyogi D, Melillo J (2015) Evapotranspiration in Northern Eurasia: impact of forcing uncertainties on terrestrial ecosystem model estimates. J Geophys Res 120(7):2014JD022531

Ojima DS, Chuluun T (2008) Implications for land use and landscapes. In: Galvin KA, Reid RS, Behnke JRH, Hobbs NT (eds) Fragmentation in semi-arid and arid landscapes: consequences for human and natural systems. Springer, New York, pp 179–193

Olson DM, Dinerstein E, Wikramanayake ED, Burgess ND, Powell GVN, Underwood EC, D'Amico JA, Itoua I, Strand HE, Morrison JC, Loucks CJ, Allnutt TF, Ricketts TH, Kura Y, Lamoreux JF, Wettengel WW, Hedao P, Kassem KR (2001) Terrestrial ecoregions of the world: a new map of life on earth. Bioscience 51(11):933–938

Park H-S, Sohn BJ (2010) Recent trends in changes of vegetation over East Asia coupled with temperature and rainfall variations. J Geophys Res 115(D14):D14101

Pederson N, Leland C, Nachin B, Hessl AE, Bell AR, Martin-Benito D, Saladyga T, Suran B, Brown PM, Davi NK (2013) Three centuries of shifting hydroclimatic regimes across the Mongolian Breadbasket. Agric For Meteorol 178–179:10–20

Pederson N, Hessl AE, Baatarbileg N, Anchukaitis KJ, Di Cosmo N (2014) Pluvials, droughts, the Mongol Empire, and modern Mongolia. Proc Natl Acad Sci USA 111(12):4375–4379

Piao S, Mohammat A, Fang J, Cai Q, Feng J (2006) NDVI-based increase in growth of temperate grasslands and its responses to climate changes in China. Glob Environ Change 16(4):340–348

Poulter B, Pederson N, Liu H, Zhu Z, D'Arrigo R, Ciais P, Davi N, Frank D, Leland C, Myneni R, Piao S, Wang T (2013) Recent trends in Inner Asian forest dynamics to temperature and precipitation indicate high sensitivity to climate change. Agric For Meteorol 178–179:31–45

Poulter B, Frank D, Ciais P, Myneni RB, Andela N, Bi J, Broquet G, Canadell JG, Chevallier F, Liu YY, Running SW, Sitch S, van der Werf GR (2014) Contribution of semi-arid ecosystems to interannual variability of the global carbon cycle. Nature 509(7502):600–603

Prince SD, Wessels KJ, Tucker CJ, Nicholson SE (2007) Desertification in the Sahel: a reinterpretation of a reinterpretation. Glob Change Biol 13(7):1308–1313

Qi J, Jiquan C, Shiqian W, Likun A (2012) Understanding the coupled natural and human systems in Dryland East Asia. Environ Res Lett 7(1):015202

Reynolds JF, Smith DMS, Lambin EF, Turner BL, Mortimore M, Batterbury SPJ, Downing TE, Dowlatabadi H, Fernández RJ, Herrick JE, Huber-Sannwald E, Jiang H, Leemans R, Lynam T, Maestre FT, Ayarza M, Walker B (2007) Global desertification: building a science for dryland development. Science 316(5826):847–851

Rienecker MM, Suarez MJ, Gelaro R, Todling R, Bacmeister J, Liu E, Bosilovich MG, Schubert SD, Takacs L, Kim G-K, Bloom S, Chen J, Collins D, Conaty A, da Silva A, Gu W, Joiner J, Koster RD, Lucchesi R, Molod A, Owens T, Pawson S, Pegion P, Redder CR, Reichle R, Robertson FR, Ruddick AG, Sienkiewicz M, Woollen J (2011) MERRA: NASA's modern-era retrospective analysis for research and applications. J Clim 24(14):3624–3648

Runnström MC (2000) Is Northern China winning the battle against desertification? Ambio 29(8):468–476

Samanta A, Ganguly S, Vermote E, Nemani RR, Myneni RB (2012) Interpretation of variations in MODIS-measured greenness levels of Amazon forests during 2000–2009. Environ Res Lett 7(2):024018

Sankey TT, Sankey JB, Weber KT, Montagne C (2009) Geospatial assessment of grazing regime shifts and sociopolitical changes in a Mongolian Rangeland. Rangel Ecol Manag 62(6):522–530

Scheftic W, Zeng X, Broxton P, Brunke M (2014) Intercomparison of seven NDVI products over the United States and Mexico. Remote Sens 6(2):1057

Sen PK (1968) Estimates of the regression coefficient based on Kendall's Tau. J Am Stat Assoc 63(324):1379–1389

Sharkhuu A, Plante A, Enkhmandal O, Casper B, Helliker B, Boldgiv B, Petraitis P (2013) Effects of open-top passive warming chambers on soil respiration in the semi-arid steppe to taiga forest transition zone in Northern Mongolia. Biogeochemistry 115(1–3):333–348

Tucker CJ (1979) Red and photographic infrared linear combinations for monitoring vegetation. Remote Sens Environ 8(2):127–150

Wang J, Brown D, Chen J (2013a) Drivers of the dynamics in net primary productivity across ecological zones on the Mongolian Plateau. Landscape Ecol 28(4):725–739

Wang J, Brown DG, Agrawal A (2013b) Climate adaptation, local institutions, and rural livelihoods: a comparative study of herder communities in Mongolia and Inner Mongolia, China. Glob Environ Change 23(6):1673–1683

Wessels KJ, Prince SD, Malherbe J, Small J, Frost PE, VanZyl D (2007) Can human-induced land degradation be distinguished from the effects of rainfall variability? A case study in South Africa. J Arid Environ 68(2):271–297

Wessels KJ, van den Bergh F, Scholes RJ (2012) Limits to detectability of land degradation by trend analysis of vegetation index data. Remote Sens Environ 125:10–22

Wright C, de Beurs K, Henebry G (2012) Combined analysis of land cover change and NDVI trends in the Northern Eurasian grain belt. Front Earth Sci 6(2):177–187

Xiao J, Moody A (2004) Trends in vegetation activity and their climatic correlates: China 1982–1998. Int J Remote Sens 25(24):5669–5689

Xiao J, Moody A (2005) Geographical distribution of global greening trends and their climatic correlates: 1982–1998. Int J Remote Sens 26(11):2371–2390

Yuan C, Liu S, Xie N (2010) The impact on chinese economic growth and energy consumption of the Global Financial Crisis: an input–output analysis. Energy 35(4):1805–1812

Zhang C, Li W, Fan M (2013) Adaptation of herders to droughts and privatization of rangeland-use rights in the arid Alxa Left Banner of Inner Mongolia. J Environ Manag 126:182–190

Zhao X, Hu H, Shen H, Zhou D, Zhou L, Myneni R, Fang J (2014) Satellite-indicated long-term vegetation changes and their drivers on the Mongolian Plateau. Landscape Ecol. doi:10.1007/s10980-014-0095-y